LUMINESCENCE SENSING OF STRESS IN COMPOSITE STRUCTURES

H.J. Hough, J.N. Demas*, and H.N.G. Wadley
Intelligent Processing of Materials Laboratory
School of Engineering and Applied Science
University of Virginia
Charlottesville, VA 22903

INTRODUCTION

High temperature composites utilizing ceramic fibers (e.g. SiC or Al_2O_3) and high melting point metals, intermetallics, and ceramics are being developed for applications in aircraft turbine engines, air frames, and the skins of hypersonic vehicles [1]. In order to achieve the strength necessary for these applications, single crystal Al_2O_3 (sapphire) reinforcing fibers are used because of their combination of very high modulus (~450 GPa), low density (~3.7 g cm^{-1}), excellent low temperature strength (3-4 GPa), exceptionally good creep strength, and chemical stability in oxidizing environments.

The doping of these single crystals (during either growth or by subsequent high temperature diffusion annealing) with a small concentration of chromium (e.g. 0.05wt%Cr) results in the formation of ruby with no degradation in the fiber's mechanical properties. (It may even improve creep resistance.) Ruby has been known for many years to luminesce in the red following irradiation in the blue/green region of the spectrum. The luminescence spectrum contains several strong, narrow peaks. The wavelength of the luminescence peaks are a function of stress and temperature in the crystal [2]. The strong, almost linear relation between stress and wavelength (or frequency) of the luminescence peaks of ruby has been widely exploited as a method of pressure sensing during very high pressure (>1 GPa) experiments in diamond anvil cells. The technique was pioneered in the early 1970s at the National Institute of Standards and Technology (formerly NBS) by Gasper Piermarini, Stanley Block, and their coworkers [3,4]. More recently, Clarke, et al have used it to investigate local stresses in alumina ceramics [5].

The existence of luminescence in fibers that are used for reinforcement of composites provides exciting possibilities for sensing stresses through the observation and measurement of their luminescence. Using simple fiber optic coupling to the exposed end faces of fibers embedded within a high performance composite, it may be possible to nonintrusively measure the stress supported by the structural fibers without resorting to the use of foreign (e.g. silica) probe fibers that can act as sites of damage nucleation [6].

*Department of Chemistry, College of Arts and Sciences

Review of Progress in Quantitative Nondestructive Evaluation, Vol. 12
Edited by D.O. Thompson and D.E. Chimenti, Plenum Press, New York, 1993

In the work reported here, we have sought to investigate this idea. Model $Al_2O_3:Cr^{3+}$ fibers embedded in titanium matrix composites have been carefully fabricated. A high resolution, fiber optical coupled spectrometer has been assembled and used to measure the luminescence of the ruby fiber. The shifts in wavelength due to process-induced thermal residual stresses have been precisely measured and compared with elastic-plastic predictions of the fiber stress. The results suggest that the approach does indeed show considerable promise for the measurement of fiber stress in high performance composites.

PRINCIPLES OF LUMINESCENCE

Luminescence arises from a radiative (emission of a photon) transition between two states of a system. The conditions for emission are rather stringent and only a relatively small percentage of molecules are luminescent. The two types of luminescence, fluorescence and phosphorescence, are characterized by the multiplicities of the ground and the emitting states. Fluorescence is characterized by initial and final states of the same multiplicity. For fluorescence, the transition is thus not forbidden by spin selection rules; therefore, it is highly allowed and short lived (typically nanoseconds). Phosphorescence, on the other hand, involves a spin flip or change of multiplicity between the excited and ground states. Formally, such transitions are forbidden, but in practice various mechanisms relieve the forbiddeness of the transition and make it somewhat allowed. This forbiddeness causes phosphorescence to have long lifetimes in the hundreds of microseconds to seconds range. Chromium(III) has a quartet ground state and quartet and doublet excited states. In this case fluorescence is a quartet-quartet process and phosphorescence is a doublet-quartet transition. (In ruby, only phosphorescence is observed.) Even when excitation is into upper excited states, emission is still usually from the lowest excited states. Radiationless decay from the upper states to the emitting states proceeds by a series of small steps with loss of energy to the environment as heat until the lowest excited states are reached.

The addition of chromium(III) (with three outer d-electrons, designated d^3) to Al_2O_3 to form ruby leads to the incorporation of Cr^{3+} in near octahedral sites of the Al_2O_3 (trigonal symmetry) lattice. The octahedral crystal field of the unstrained lattice splits the 5-fold degenerate d-orbitals of the free ion into a (lower energy) 3-fold degenerate t_{2g} orbital and an upper e_g orbital. The notation, from group theory, is for an octahedral point group, where the "g" subscript denotes an orbital that is symmetric with respect to inversion (gerade); all d-electron derived excited states will be g in a centrosymmetric point group. The three d-electrons of Cr^{3+} will occupy the three t_{2g} d-orbitals in the unstrained lattice. Our description of the optical spectroscopy of ruby builds on the orbital and state diagram of an ion in such an octahedral site (see Figure 1). This d^3 configuration gives rise to a $^4A_{2g}$ ground state. Excited states arise from spin flips within the t_{2g} orbital and promotions with or without spin flips of a t_{2g} electron to an e_g orbital. The excited t_{2g} configuration yields doublet excited states including a ^2E_g state, which is the lowest excited state in the ion; the ruby phosphorescence arises from the $^2E_g \rightarrow {}^4A_{2g}$ transition. Since this transition is formally spin forbidden, the ruby phosphorescence is also forbidden and is therefore long-lived (several milliseconds). Similarly, direct absorption to this state ($^2E_g \leftarrow {}^4A_{2g}$) is forbidden, and the transition is too weak to pump effectively. Two quartet excited states ($^4T_{1g}$ and $^4T_{2g}$) arising from the $t_{2g}^2 e_g$ configuration give rise to allowed absorptions ($^4T_{1g} \leftarrow {}^4A_{2g}$ and $^4T_{2g} \leftarrow {}^4A_{2g}$). These allowed transitions in the blue and green parts of the spectrum give ruby its red color and absorb intensely enough to be pumped efficiently by a variety of lasers including ionized Ar, HeCd, and green HeNe. Once excited, the $^4T_{1g}$ and $^4T_{2g}$ states decay nonradiatively with unit efficiency to the lower ^2E_g state, which then emits the luminescence of interest.

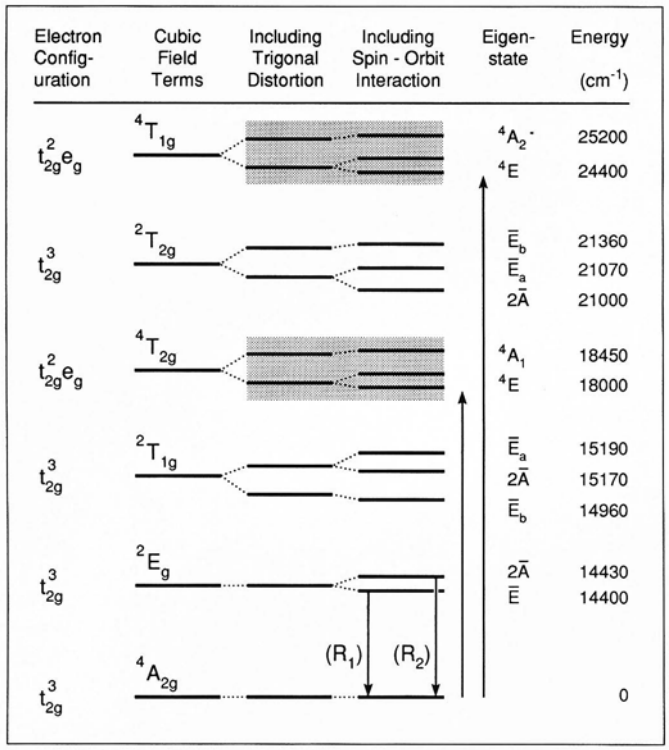

Figure 1. Energy levels for Cr^{3+} in Al_2O_3 lattice. Transitions from the $\overline{2A}$ and $\overline{E}$ excited states to the $^4A_{2g}$ ground state results in the R2 and R1 ruby luminescence lines, respectively. Excitation to the shaded levels can be accomplished using blue/green light.

The picture is actually a little more complicated than presented above. The Cr^{3+} is located in a site with a slight trigonal distortion. This distortion, together with spin–orbit coupling, splits the ^2E_g state into an $\overline{E}$ and a $\overline{2A}$ state separated in energy by about 30 cm^{-1}. Our notation now switches to those used for spin orbit states in the noncentrosymmetric trigonal crystal field. These two nearly-degenerate states give rise to the ruby doublet in the phosphorescence spectrum, designated R1 and R2. In the absence of an externally imposed lattice strain, these states are 14402 cm^{-1} and 14430 cm^{-1} above the ground state. Decay, via radiative transitions, thus results in luminescence with two spectral lines (the R1 and R2 lines, respectively) with wavelengths of approximately 693 nm and 694 nm (see Fig. 1).

Grabner has calculated the relationship between the scalar lineshift of the R1 line and the individual components of the stress tensor [8]:

$$\Delta\nu=\Pi_{11}(\sigma_{11}+\sigma_{22}+\sigma_{33})+(\Pi_{33}-\Pi_{11})(a_{31}^2\sigma_{11}+a_{32}^2\sigma_{22}+a_{33}^2\sigma_{33})$$
$$+2(\Pi_{33}-\Pi_{11})(a_{31}a_{32}\sigma_{12}+a_{31}a_{33}\sigma_{13}+a_{32}a_{33}\sigma_{23}) \quad (1)$$

where $\Delta\nu$ is the line shift in cm^{-1}, Π_{ij} are the piezospectroscopic coefficients, σ_{mn} are the stress components, and $a_{im}a_{jn}$ represent the orthogonal transformation between the crystal coordinates and the principle stress axes. From a measurement of $\Delta\nu$, one can infer information about the stress in a chromium doped Al_2O_3 fiber provided one has numerical values for the piezospectroscopic constants and the fiber orientation is known. If the

resolution of stress is determined by the line shift error (0.4 cm^{-1}), the smallest stress detectable by the method is ~200 MPa--a value of significance to those concerned with optimizing the stress in composites.

EXPERIMENTAL

We have initially studied two metal matrix composite samples. Each was made by stacking commercially pure titanium matrix foils on either side of three widely spaced 200 μm diameter ruby fibers. The fibers in one sample were obtained from Lasergenics Corp. They were grown by the laser pedestal method [9] and were doped with 0.05wt% Cr(III). The fibers in the second sample were supplied by Saphikon, Inc. They were grown by the edge defined film fed growth technique [10] and contained 0.03wt% Cr(III). Each composite's final size was 2 cm x 2 cm x 1.5 mm. They were then placed in stainless steel containers which had been coated with boron nitride for easy release and were HIP consolidated at 900 °C and 100 MPa for one hour. They were cooled at a rate of 4.3 °C/min. and simultaneously depressurized at a rate of 0.644 MPa/min. down to 250 °C and 500 psi, from which point the HIP was vented to room temperature and pressure.

Each can was removed and the samples were sectioned with a diamond wheel and polished to improve optical transmission through the fiber ends. Luminescence was excited in the fibers by propagating the 514.5 nm line of an Omnichrome argon ion laser through a $CuSO_4$ solution filter to remove any red plasma emissions, a 5 cm focal length lens, and a bifurcated fiber optic bundle (Fig. 2). A 0.64 m monochromator made by Instruments, SA, dispersed the resulting luminescence signal and focused it onto a liquid nitrogen cooled charge coupled device. We obtained the luminescence spectra from both fibers that had been embedded in a matrix and fibers that had not been embedded in a matrix. The peak wavelength of each spectrum was then determined using the PRISM software program supplied from Instruments, SA. The reproducibility of a peak's wavelength was ±0.17 Å (0.3 cm^{-1}). All measurements were made at ambient temperature.

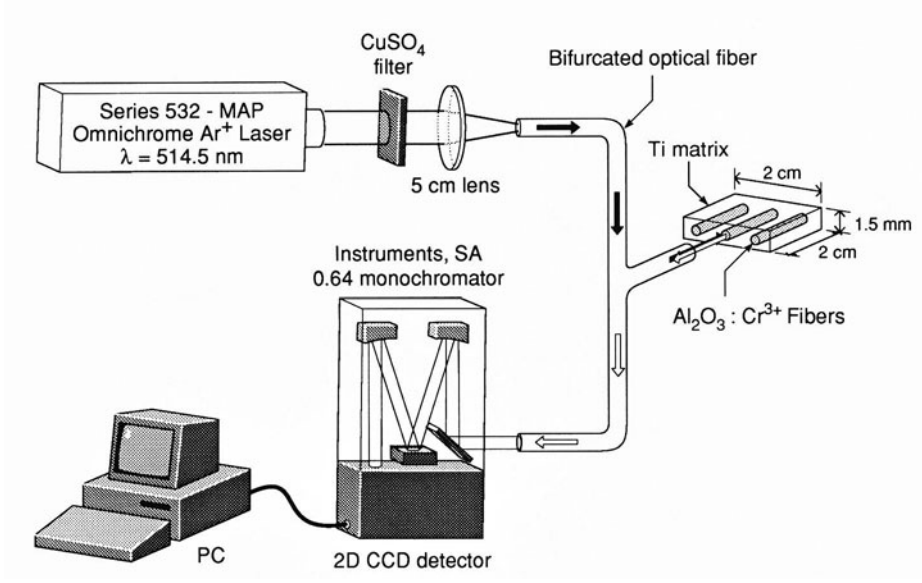

Figure 2. Schematic diagram of system to measure luminescence wavelength.

RESULTS

Figure 3 shows a typical spectrum from composited and uncomposited 0.05wt% Cr(III) doped fibers. Two phosphorescence spectral peaks (R1 and R2) are shown. Note the shift in the peak positions associated with compositing. The R1 peak shift was measured for all six of the fibers and is shown in Table 1 together with the average value for each of the two samples.

DISCUSSION

The results show a substantial shift in the R1 line luminescence wavelength has occurred upon compositing. For c-axis fibers the relationship between the shift and the components of fiber stress can be derived from equation (1)

$$\Delta\nu = \Pi_{11}(\sigma_{11} + \sigma_{22}) + \Pi_{33}\sigma_{33} \qquad (2)$$

Assuming the stresses are due only to differential thermal contractions between the titanium matrix and the aluminum oxide fiber upon cooling, we can calculate the stress components from concentric cylinder models [11,12,13]. Using the recent elastic-plastic model of Pindera [13] and the thermophysical constants of Al_2O_3 and titanium given in Table 2, we obtain equal radial and hoop stresses (σ_{11} and σ_{22}) of -269 MPa and an axial stress (σ_{33}) of 1.13 GPa for ΔT=-880 °C (Fig. 4). Substituting these into equation (2) and using

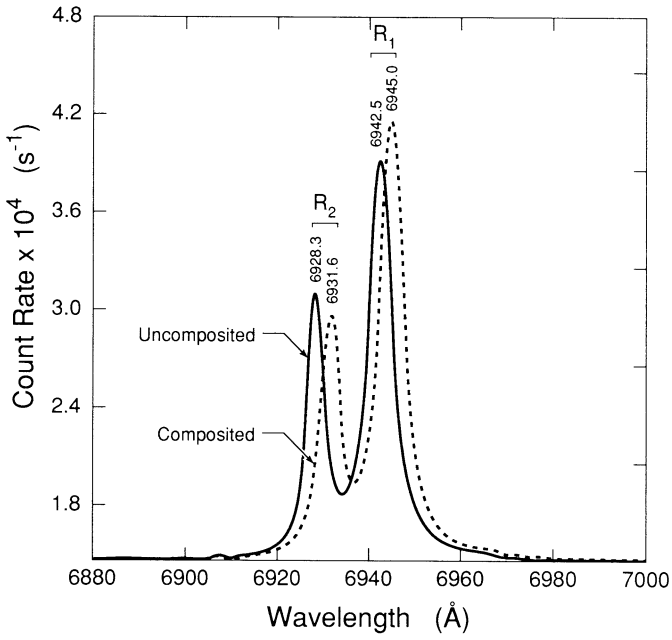

Figure 3. Peak shifts for composited and uncomposited fibers.

Table 1. Lineshifts for 0.03wt% Cr-doped fibers (left column) and 0.05wt% Cr-doped fibers (right column).

	$\Delta\bar{\nu}_{03}$ (cm^{-1})	$\Delta\bar{\nu}_{05}$ (cm^{-1})
Fiber 1	-2.9± 0.3	-2.8± 0.4
Fiber 2	-4.9± 0.3	-4.2± 0.4
Fiber 3	-2.8± 0.3	-4.9± 0.4
Average	-3.5	-4.0

Table 2. Thermophysical values used in residual stress calculation.

Titanium

Temp (°C)	E (MPa)	α ($x10^{-6}°C^{-1}$)	YP (MPa)
900	40.4	10.4	116
700	55.7	10.1	116
500	70.9	9.8	117
300	86.4	9.5	190
100	101.4	9.0	396
24	107.2	8.7	571

ν=0.36 HSP=2 GPa

Aluminum Oxide

Temp (°C)	E (MPa)	α_{zz}($x10^{-6}°C^{-1}$)	α_{rr}($x10^{-6}°C^{-1}$)
900	268	13.7	11.4
700	294	13.1	10.9
500	313	12.1	9.8
300	326	9.5	8.1
100	335	6.2	5.8
24	338	5.4	5.4

ν=0.33

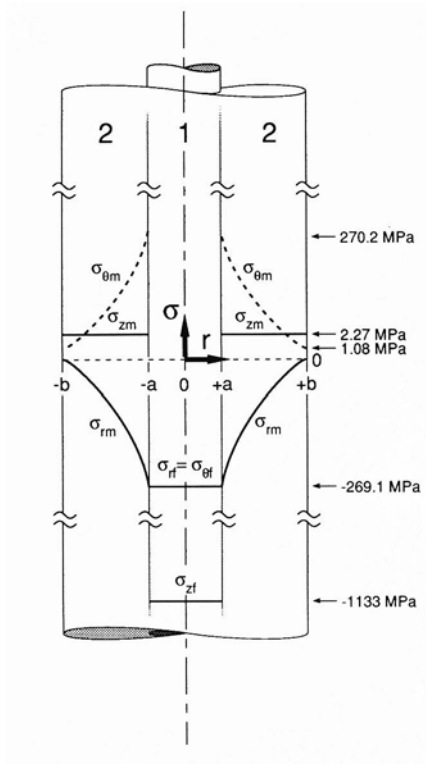

Figure 4. Schematic diagram of stresses in the fiber (material 1) and the matrix (material 2).

Π_{11}=3.0 cm^{-1} and Π_{33}=1.8 cm^{-1} [12], results in a calculated line shift of $\Delta\nu_c$=-3.65 cm^{-1}. Comparison with the values given in Table 1 are in approximate agreement with the average shifts of the three fibers in each sample but there are significant differences between individual fibers.

An analysis of our experimental errors indicates a precision in measured wavelength shift of 0.4 cm^{-1}. This is less than the shift differences observed between the different fibers. Thus, we conclude that either the piezospectroscopic constants vary from fiber to fiber, or the fibers are under slightly different stresses. There could be several reasons that might cause a variation in stress. These include pre-existing fiber stresses (before compositing), stresses induced by thermal mismatch strains between the sample and its can material and nonuniformity in temperature during cooling. These and other possible effects will be investigated in future work. Nevertheless, it appears that the technique has considerable merit for the determination of fiber stress.

ACKNOWLEDGEMENTS

The authors wish to thank Jerry Fitzgibbon of Saphikon, Inc., for providing ruby fibers for us, and gratefully acknowledge the assistance of Todd Williams of the University of Virginia for performing the thermal stress calculations. We are very grateful to D.R. Clarke and A. Evans of UCSB and D. Backman of GE Aircraft Engines for their encouragement and helpful discussion of the approach. This work was funded by the Academic Enhancement Program of the University of Virginia and the Defense Advanced Research Projects Agency through a joint NASA/DARPA program and the DARPA funded UCSB University Research Initiative.

REFERENCES

1. J.R. Stephens,"High Temperature Metal Matrix Composites for Future Aerospace Systems,"NASA TM-100212, Springfield,VA: National Technical Information Service,1987.
2. J.D. Barnett, et al, Rev.Sci.Instr., 44,1(1973).
3. R.A. Forman, et al, Science,176,284(1972).
4. G.J. Piermarini, et al, J.Appl.Phys.,46,6,2774(1975).
5. S.E. Molis and D.R. Clarke, J.Am.Cer.Soc.,73,3189(1990).
6. B. Culshaw and J. Dakin,*Optical Fiber Sensors: Systems and Applications*,vol.2 (Artech House,Inc., Norwood,MA, 1989).
7. A.L. Schawlow in *Advances in Quantum Electronics*,edited by J.R. Singer(Columbia University Press, 1961).
8. L. Grabner, J.Appl.Phys.,49,580(1978).
9. M.M. Fejer, et al, Rev.Sci.Instr.,55,11(1984).
10. D.G. Backman, et al, in *Advanced Sensing, Modelling, and Control of Materials Processing*,edited by E.F. Matthys and B. Kushner (The Minerals,Metals and Materials Society, Warrendale,PA,1992).
11. K.K. Chawla, *Composite Materials* (Springer-Verlag,New York,1987).
12. R.P. Nimmer, J.Comp.Tech.Res.,12,65(1990).
13. M-J. Pindera, Comp.Eng.,1,69(1991).